Spin Coupling and Orbital Angular Momentum Quenching in Free Iron Clusters

M. Niemeyer,[1,2] K. Hirsch,[1,2] V. Zamudio-Bayer,[1,2] A. Langenberg,[1,2] M. Vogel,[1] M. Kossick,[1,2] C. Ebrecht,[1,2] K. Egashira,[3] A. Terasaki,[4,5] T. Möller,[2] B. v. Issendorff,[6] and J. T. Lau[1,*]

[1]*Institut für Methoden und Instrumentierung der Forschung mit Synchrotronstrahlung, Helmholtz-Zentrum Berlin für Materialien und Energie GmbH, Albert-Einstein-Straße 15, 12489 Berlin, Germany*

[2]*Institut für Optik und Atomare Physik, Technische Universität Berlin, Hardenbergstraße 36, 10623 Berlin, Germany*

[3]*East Tokyo Laboratory, Genesis Research Institute, Inc., 717-86 Futamata, Ichikawa, Chiba 272-0001, Japan*

[4]*Cluster Research Laboratory, Toyota Technological Institute, 717-86 Futamata, Ichikawa, Chiba 272-0001, Japan*

[5]*Department of Chemistry, Kyushu University, 6-10-1 Hakozaki, Higashi-ku, Fukuoka 812-8581, Japan*

[6]*Fakultät für Physik, Universität Freiburg, Stefan-Meier-Straße 21, 79104 Freiburg, Germany*

(Received 16 October 2011; published 30 January 2012)

Magnetic spin and orbital moments of size-selected free iron cluster ions Fe_n^+ ($n = 3$–20) have been determined via x-ray magnetic circular dichroism spectroscopy. Iron atoms within the clusters exhibit ferromagnetic coupling except for Fe_{13}^+, where the central atom is coupled antiferromagnetically to the atoms in the surrounding shell. Even in very small clusters, the orbital magnetic moment is strongly quenched and reduced to 5%–25% of its atomic value while the spin magnetic moment remains at 60%–90%. This demonstrates that the formation of bonds quenches orbital angular momenta in homonuclear iron clusters already for coordination numbers much smaller than those of the bulk.

DOI: 10.1103/PhysRevLett.108.057201 PACS numbers: 75.75.−c, 36.40.Cg, 75.30.Cr, 75.50.Bb

As atoms, most elements with open shells carry spin and orbital magnetic moments, which are typically a few Bohr magneton. In bulk form, only a few elements are ferromagnetically ordered, with iron, cobalt, and nickel as the most prominent examples. Even in these $3d$ ferromagnets the orbital magnetic moment is quenched by the symmetry of the crystal lattice, which mixes wave functions with equal contributions of the magnetic quantum number $\pm m_l$ to yield an orbital angular momentum of $\langle l_z \rangle = 0$. Spin-orbit coupling can restore the orbital magnetic moment, but this is a small effect in $3d$ transition metals. As a consequence, the total magnetic moment is almost pure spin moment in these systems, and the orbital magnetic moment amounts to only 5%–10% of its atomic value. While a quantitative treatment of the orbital magnetic moment is still a challenge for theory, it is accessible in experiment, where spin and orbital magnetic moments can be determined by x-ray magnetic circular dichroism spectroscopy [1–3]. When applied to surfaces [4], ultrathin films [5], deposited clusters [6,7], monoatomic chains [8], or adatoms [9], it is seen that orbital magnetic moments can be strongly enhanced over the bulk value by environments of reduced symmetry, while the relative enhancement of the spin moment is less pronounced. By extrapolation of these results, one could thus expect that in small clusters, which form a link between single atoms and low-dimensional nanostructures, the orbital moment constitutes a significant contribution to the total magnetic moment. On the other hand, free clusters usually adopt compact structures where the local environment is different for each atom. Typically, such a cluster does not possess a clearly preferred global axis along which the individual orbital moments could be restored by spin-orbit coupling, but different axes for each site. This should lead to strongly reduced average orbital moments.

So far, magnetic moments of isolated clusters have only been determined in Stern-Gerlach experiments [10–13], which find increased total magnetic moments but cannot discriminate between spin and orbital contributions. For the smallest Fe_n clusters studied in a Stern-Gerlach setup, $n = 10$–12, average magnetic moments larger than the atomic spin moment were found experimentally [12], indicating strong contributions of unquenched orbital magnetic moments. To address the question of whether and how orbital moments are quenched, and to separate spin and orbital contributions to the total magnetic moment, we have applied x-ray circular magnetic dichroism spectroscopy [1–3] to size-selected iron cluster ions. In contrast to previous results [12], our findings demonstrate that orbital magnetic moments are strongly quenched already for clusters of only three atoms.

X-ray magnetic circular dichroism spectroscopy of size-selected cluster ions was performed in ion yield mode at $T = 10$–20 K and $B = 0$–5 T in a linear radio-frequency ion trap [14–16], modified for liquid helium cooling and situated in the homogeneous magnetic field of a superconducting solenoid [17]. Iron clusters were generated by a magnetron gas aggregation source and size selected with a radio-frequency quadrupole mass filter. They were guided by a combination of electrostatic ion optics and radio-frequency multipole ion guides into the ion trap where circularly polarized x-ray photons from an undulator beam line are coupled in on axis. Inside the cryogenic ion trap, and with the magnetic field applied, size-selected

cluster ions are thermalized by collisions with a helium buffer gas which acts as a heat bath and is permanently present during the experiment. Ion yield spectra [14–16,18] of $2p \rightarrow 3d$ excitation in Fe_n^+ clusters were recorded for parallel and antiparallel alignment of photon helicity $\boldsymbol{\sigma}$ and magnetic field $\boldsymbol{B}$ with a time-of-flight mass spectrometer. All spectra are normalized to incident photon flux, recorded *in situ* with a GaAsP photodiode located behind the ion trap, and x-ray magnetic circular dichroism spectra were corrected for a 90% degree of circular polarization.

X-ray magnetic circular dichroism sum rules [1–3] allow us to derive expectation values of $3d$ electron orbital angular momentum $\langle L_z \rangle$ and spin angular momentum plus magnetic dipole contribution $\langle S_z \rangle + 7/2\langle T_z \rangle$ from absorption intensities of $2p \rightarrow 3d$ transitions for parallel (μ_+) and antiparallel (μ_-) alignment of magnetic field $\boldsymbol{B}$ and helicity $\boldsymbol{\sigma}$ of circularly polarized x-ray photons. X-ray magnetic circular dichroism spectra $\mu_+ - \mu_-$ of Fe_n^+ are shown in Fig. 1 to illustrate the quality of the data at typical target densities of 5×10^7 ions per cm^3 along the 20 cm interaction region, corresponding to 10^9 ions per cm^2 or 10^{-5} atomic monolayer equivalent. For ease of comparison, these spectra are normalized to the integrals of the corresponding isotropic x-ray absorption spectra $1/2(\mu_+ + \mu_-)$ to account for the number of absorbing atoms and transition intensities, as well as Brillouin corrected to account for nonsaturation magnetization at $B = 5$ T and $T = 15$–20 K.

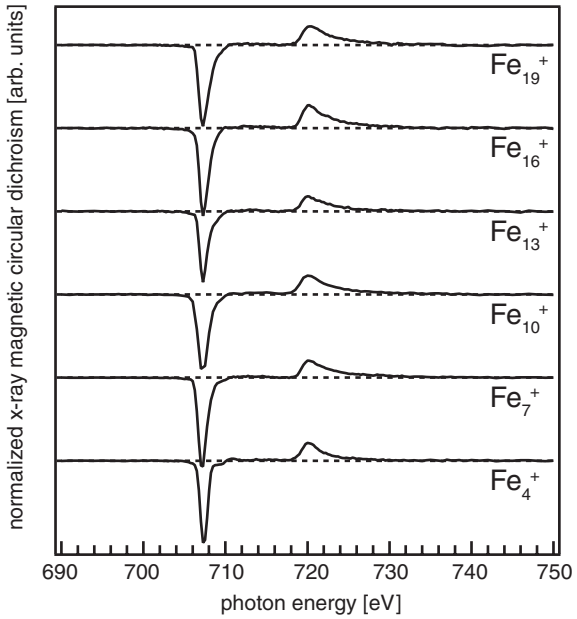

FIG. 1. X-ray magnetic circular dichroism spectra of trapped Fe_n^+ clusters, recorded at $B = 5$ T and $T = 15$–20 K. All spectra are normalized, Brillouin corrected, and shown on the same scale for comparison.

To calculate per atom values of spin (μ_S) and orbital (μ_L) magnetic moments from x-ray magnetic circular dichroism sum rules [1–3], the number n_h of unoccupied $3d$ states is required. For iron clusters, $n_h = 3.3 \pm 0.2$ is assumed, which is the average of $n_h = 3.25$ predicted for Fe_2^+ [19], $n_h = 3.15$–3.48 for Fe_n clusters [20], and $n_h = 3.34$–3.44 for bcc iron [20,21]. The small scatter of these predicted values as well as the close agreement of n_h for the limiting cases of Fe_2^+ and bcc iron show that no large variation of n_h is to be expected even for small iron clusters.

Magnetization curves of Fe_n^+ clusters at fixed ion trap temperature were obtained by recording x-ray magnetic circular dichroism spectra at different values of the applied magnetic field. For Fe_{10}^+, such a magnetization curve is shown in Fig. 2. The curve indicates superparamagnetic behavior [22] and yields a saturation magnetization of $\mu_J = 3.5 \pm 0.2\ \mu_B$ per atom as well as an ion temperature of $T = 13 \pm 2$ K when fitted with a Brillouin function. Magnetization curves can thus be used to determine the cluster ion temperature, which is typically a few kelvin higher than the ion trap temperature reading because of radio-frequency heating. To calibrate ion temperatures, magnetization curves were recorded for Fe_{10}^+, Fe_{14}^+, and Fe_{15}^+. For all other Fe_n^+ clusters presented here, spin and orbital magnetizations were determined at maximum magnetic field, $B = 5$ T, and at fixed ion temperatures in the range of $T = 15$–20 K. Since these experimental conditions correspond to the Zeeman (weak-field) limit for $3d$ transition metals, the total magnetic moment $\mu_J = \mu_S + \mu_L$ is aligned by the applied magnetic field, and saturation magnetic moments μ_S and μ_L were derived with the Brillouin correction factor obtained for μ_J of a given Fe_n^+ cluster.

In Fig. 3, spin, orbital, and total magnetic moments of Fe_n^+ clusters are shown per unoccupied $3d$ state (left axis) and per atom (right axis) for $n = 3$–20. With the exception

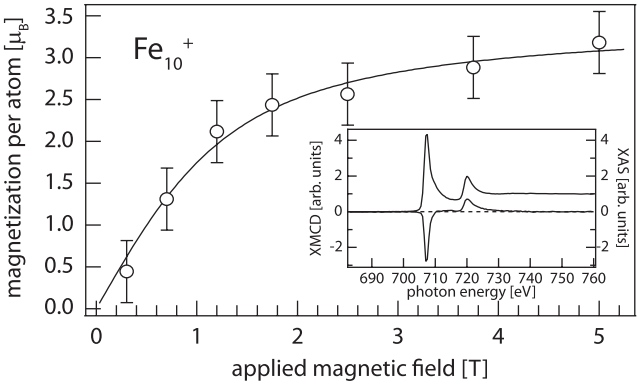

FIG. 2. Magnetization curve of Fe_{10}^+ clusters. The fit with a Brillouin curve yields a saturation magnetization of $\mu_J = 3.5 \pm 0.2\ \mu_B$ per atom and a cluster temperature of $T = 13 \pm 2$ K. The inset shows x-ray absorption (XAS) and x-ray magnetic circular dichroism (XMCD) spectra of Fe_{10}^+ at $B = 5$ T.

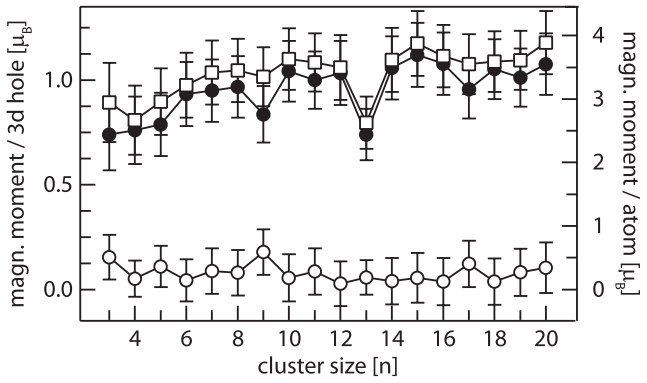

FIG. 3. Spin (filled circles), orbital (open circles), and total (boxes) magnetic moments per 3*d* hole (left axis) and per atom (right axis) of Fe_n^+ clusters. In Fe_{13}^+, antiferromagnetic coupling of the central atom to the surrounding shell and reduced spin magnetic moments [23,24,32] lead to a significantly lower total magnetic moment.

of Fe_{13}^+, magnetic spin moments are $\mu_S \approx 1\ \mu_B$ per unoccupied 3*d* state for $n \geq 6$. This is a sign of completely filled majority spin states; i.e., these states are located below the Fermi energy for iron clusters in contrast to bulk iron. A possible reason for this behavior is 3*d* band narrowing because of the reduced average coordination number in small iron clusters.

Total magnetic moments of $\mu_J = 3.2$–$3.9\ \mu_B$ per atom for $n \geq 6$ agree well with results of Stern-Gerlach experiments [11–13] of iron clusters, which find $\mu_J \approx 3\mu_B$ for 25–150 atoms per cluster, as well as with theoretical predictions of $\mu_S \approx 3.0$–$3.5\ \mu_B$ per atom [23–28]. This agreement implies that there is no significant contribution of the anisotropic magnetic dipole term $\langle T_z \rangle$ to the spin sum rule in the x-ray magnetic circular dichroism data of iron cluster ions presented here. There are two possible explanations: On the one hand, it seems reasonable that $\langle T_z \rangle$ is much smaller than usually found, e.g., at surfaces, since free clusters do not possess clearly preferred axes. On the other hand, however, even a strong contribution of $\langle T_z \rangle$ to the spin sum rule [1–3] vanishes if x-ray magnetic circular dichroism is performed either in a magic angle geometry on an oriented sample or averaged over random spatial orientations as in polycrystalline samples [5,29]. For free clusters magnetized in an external magnetic field, such random orientations can only occur if the clusters are allowed to rotate while their magnetic moments remain aligned along the magnetic field. This is the case if the magnetocrystalline anisotropy energy E_{MAE} is smaller than the rotational energy for a given axis, i.e., $E_{\mathrm{MAE}} \leq 1/2k_BT$. Otherwise, strong coupling of the magnetic moment to an easy magnetization axis would hinder cluster rotation and lead to lattice orientation along this preferred axis. Further evidence for random spatial orientation can be inferred from x-ray absorption spectra $1/2(\mu_+ + \mu_-)$ recorded for one cluster size at different values of the applied magnetic field: If the magnetocrystalline anisotropy energy E_{MAE} was strong, the applied magnetic field would lead to spatial alignment of the clusters, which would result in x-ray natural linear dichroism. This was not observed under the present experimental conditions, again indicating random spatial orientation of the clusters and a small magnetocrystalline anisotropy energy $E_{\mathrm{MAE}} \leq 1/2k_BT$. From this constraint, an upper limit of the magnetocrystalline anisotropy energy $E_{\mathrm{MAE}} \leq 65\ \mu$eV per atom can be estimated for Fe_{10}^+ and $k_BT = 1.3$ meV at $T = 15$ K, corresponding to ≤ 46-fold enhancement of E_{MAE} over the bulk value of 1.4 μeV [30]. This result is consistent with the magnetic anisotropy energy of 150 μeV per atom predicted for iron dimers [31], as it can be expected that the magnetocrystalline anisotropy energy decreases with cluster size.

In the size range investigated here, an exceptionally low spin moment of $\mu_S = 2.4 \pm 0.4\ \mu_B$ is obtained experimentally for Fe_{13}^+, as can be seen in Fig. 3. In theoretical studies [23–26,32,33], neutral Fe_{13} is predicted to adopt a distorted icosahedral structure with two possible magnetic configurations: A ferromagnetic configuration [23,24,32] with an average spin magnetic moment of $\mu_S = 3.38\ \mu_B$ per atom, and a configuration where the central atom of the distorted icosahedron couples antiferromagnetically to the 12 atoms of the surrounding shell [25,26,33]. In this second case, average interatomic distances are contracted by 2%–3% [24,32,33], which reduces the spin magnetic moments in the surrounding shell and leads to an average spin moment of $\mu_S = 2.62\ \mu_B$ per atom [23,24,32]. Our experimental result of $\mu_S = 2.4 \pm 0.4\ \mu_B$ for Fe_{13}^+ gives strong evidence that this antiferromagnetically coupled configuration is the ground state of Fe_{13}^+, highlighting the subtle interdependence of magnetic coupling on atomic structure and interatomic distance [23–25,33]. For neutral Fe_{12}, predicted to be an icosahedral structure similar to Fe_{13} but with one apex atom missing [25], theoretical studies agree on a ferromagnetic ground state, but with a large scatter in average spin magnetic moments ranging from $\mu_S = 2.67\ \mu_B$ [25,26] to $\mu_S = 3.17\ \mu_B$ [23]. If one electron was removed from the minority spin states, this latter value would correspond to $\mu_S = 3.25\ \mu_B$ for Fe_{12}^+, which is close to our experimental value of $\mu_S = 3.4 \pm 0.5\ \mu_B$. The situation is similar for Fe_{14} where ferromagnetic configurations with average spin magnetic moments ranging from $\mu_S = 2.85\ \mu_B$ [26] over $\mu_S = 3\ \mu_B$ [25] to $\mu_S = 3.29\ \mu_B$ [23] are predicted. The latter high-spin value is again in close agreement with our finding of $\mu_S = 3.5 \pm 0.5\ \mu_B$ for Fe_{14}^+.

Reduced spin magnetic moments of $\mu_S = 2.4$–$2.6\ \mu_B$ per atom are also found for Fe_n^+ clusters with $n < 6$ in Fig. 3. Although counterintuitive, these decreased magnetic moments are in qualitative agreement with theoretical predictions [23,25–27] and could again be caused by contracted average nearest neighbor distances [27,32], which

are predicted to be 2.17 Å in Fe_2^+, 2.24 Å in triangular Fe_3^+, 2.29 Å in tetrahedral Fe_4^+, 2.35 Å in trigonal bipyramidal Fe_5^+, and 2.49 Å in octahedral Fe_6^+ [27]. This strong bond length contraction could overcompensate the effect of reduced coordination number in small clusters and cause a widening of the 3*d* band, i.e., a larger spread of 3*d* derived levels, which would lead to lower spin magnetic moments because of electron transfer from majority to minority states, shifted below the Fermi energy [25]. To yield further insight, high precision measurements at even lower ion temperature as well as detailed field and temperature dependent studies will have to be performed.

As shown in Fig. 3, orbital magnetic moments of Fe_n^+ clusters are strongly quenched and amount to 0.03–0.18 μ_B per 3*d* hole, or 0.1–0.6 μ_B per atom, contributing only 3%–17% to the total magnetic moment. Although a significant *relative* enhancement of the orbital magnetic moments in iron clusters up to a factor of 6 over the bulk value of 0.09 μ_B [21] is observed, the *absolute* enhancement of the orbital moment is only 0.15 μ_B per atom on average, which is small compared to the average increase of the spin moment by 1 μ_B per atom over the bulk value of 2.2 μ_B per atom [21] in the same size range.

To further illustrate the evolution of magnetic moments from atom to bulk, spin and orbital contributions of 3*d* electrons are normalized to their atomic values of $\mu_S = 4\ \mu_B$ and $\mu_L = 2\ \mu_B$, respectively, and are plotted versus $n^{-1/3} \propto 1/R$, where R is the cluster radius, in Fig. 4. Predicted 3*d* spin and orbital magnetic moments for Fe_2^+ [19] are also included in the figure and fit well into the trend from the atom to the trimer. In terms of its atomic value, the orbital angular momentum amounts only to 5%–25% for the clusters studied here, while the spin moment remains at 60%–90%. Obviously, this strong reduction of the orbital angular momentum already in Fe_3^+, predicted to be an equilateral triangle [27], is due to the formation of bonds, because of which the orbital angular momentum ceases to be a good quantum number. Only in Fe_2^+, the projection of the orbital angular momentum onto the molecular axis remains a good quantum number because of its cylindrical symmetry, resulting in the predicted orbital magnetic moment of 1 μ_B per atom [19]. Thus, experimentally observed quenching of the orbital magnetic moment in Fe_3^+ indirectly shows that its structure is indeed triangular as predicted [27].

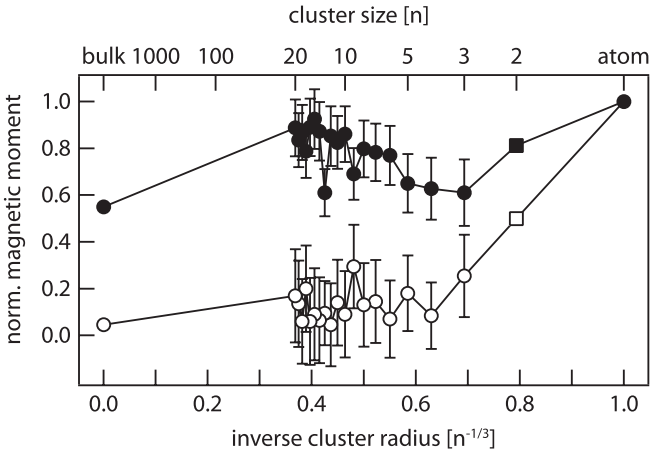

FIG. 4. Relative spin (filled circles) and orbital (open circles) magnetic moments of Fe_n^+ clusters normalized to the atomic values ($\mu_S = 4\ \mu_B$ and $\mu_L = 2\ \mu_B$). While the spin moment remains at 60%–90%, the orbital value is strongly reduced already for Fe_3^+. For Fe_2^+, calculated values (boxes) are included [19].

While there is good agreement of Fe_n^+ total magnetic moments obtained via x-ray magnetic circular dichroism with those obtained in Stern-Gerlach experiments for larger Fe_n clusters [11–13], there is a clear deviation for smaller clusters with $n \leq 12$. We find $\mu_J \approx 3.6\ \mu_B$, whereas Knickelbein reports $\mu_J \approx 4.6$–$5.4\ \mu_B$ for $n =$ 10–12 [12] and concludes an orbital contribution of $\mu_L \approx 2.4\ \mu_B$, i.e., largely unquenched magnetic orbital moments, for Fe_{12}, in contradiction to our findings. In addition to absolute values, however, upper limits of the orbital magnetic moment can be given from the ratio μ_L/μ_S, which can be determined with high accuracy from x-ray magnetic circular dichroism since uncertainties in cluster ion temperature, number of unoccupied 3*d* states, and degree of circular polarization are eliminated. From our data, we obtain $\mu_L/\mu_S = 0.05$ for Fe_{10}^+ and $\mu_L/\mu_S =$ 0.08 for Fe_{11}^+. Even a maximum spin moment of $\mu_S = 4\ \mu_B$ thus yields upper limits of $\mu_L \leq 0.21\ \mu_B$ for Fe_{10}^+ and $\mu_L \leq 0.34\ \mu_B$ for Fe_{11}^+. Hence, we can rule out strongly unquenched orbital magnetic moments in small iron clusters.

In conclusion, we have demonstrated the possibility to obtain high quality x-ray magnetic circular dichroism spectra of size-selected free cluster ions. This allows us to study spin and orbital magnetic moments of small clusters, molecules, and complexes without the perturbing effects of a surface or matrix. Performing these studies as a function of magnetic field and ion temperature has the potential to yield unprecedented insight into coupling phenomena, energies, and length scales in magnetism.

Beam time for this project was granted at BESSY II beam line UE52-SGM, operated by Helmholtz-Zentrum Berlin. Technical assistance and user support by P. Hoffmann and E. Suljoti is gratefully acknowledged. This study was partially supported by the Special Cluster Research Project of Genesis Research Institute, Inc.

*tobias.lau@helmholtz-berlin.de

[1] B. T. Thole, P. Carra, F. Sette, and G. van der Laan, Phys. Rev. Lett. **68**, 1943 (1992).

[2] P. Carra, B. T. Thole, M. Altarelli, and X. Wang, Phys. Rev. Lett. **70**, 694 (1993).

[3] C. T. Chen, Y. U. Idzerda, H.-J. Lin, N. V. Smith, G. Meigs, E. Chaban, G. H. Ho, E. Pellegrin, and F. Sette, Phys. Rev. Lett. **75**, 152 (1995).
[4] P. Gambardella, S. Rusponi, M. Veronese, S. S. Dhesi, C. Grazioli, A. Dallmeyer, I. Cabria, R. Zeller, P. H. Dederichs, K. Kern, C. Carbone, and H. Brune, Science **300**, 1130 (2003).
[5] J. Stöhr, J. Magn. Magn. Mater. **200**, 470 (1999).
[6] K. W. Edmonds, C. Binns, S. H. Baker, S. C. Thornton, C. Norris, J. B. Goedkoop, M. Finazzi, and N. B. Brookes, Phys. Rev. B **60**, 472 (1999).
[7] J. T. Lau, A. Föhlisch, R. Nietubyč, M. Reif, and W. Wurth, Phys. Rev. Lett. **89**, 057201 (2002).
[8] P. Gambardella, A. Dallmeyer, K. Maiti, M. C. Malagoli, W. Eberhardt, K. Kern, and C. Carbone, Nature (London) **416**, 301 (2002).
[9] P. Gambardella, S. S. Dhesi, S. Gardonio, C. Grazioli, P. Ohresser, and C. Carbone, Phys. Rev. Lett. **88**, 047202 (2002).
[10] D. M. Cox, D. J. Trevor, R. L. Whetten, E. A. Rohlfing, and A. Kaldor, Phys. Rev. B **32**, 7290 (1985).
[11] I. M. L. Billas, A. Châtelain, and W. A. de Heer, Science **265**, 1682 (1994).
[12] M. B. Knickelbein, Chem. Phys. Lett. **353**, 221 (2002).
[13] X. Xu, S. Yin, R. Moro, A. Liang, J. Bowlan, and W. A. de Heer, Phys. Rev. Lett. **107**, 057203 (2011).
[14] J. T. Lau, J. Rittmann, V. Zamudio-Bayer, M. Vogel, K. Hirsch, P. Klar, F. Lofink, T. Möller, and B. v. Issendorff, Phys. Rev. Lett. **101**, 153401 (2008).
[15] K. Hirsch, J. T. Lau, P. Klar, A. Langenberg, J. Probst, J. Rittmann, M. Vogel, V. Zamudio-Bayer, T. Möller, and B. von Issendorff, J. Phys. B **42**, 154029 (2009).
[16] J. T. Lau, K. Hirsch, A. Langenberg, J. Probst, R. Richter, J. Rittmann, M. Vogel, V. Zamudio-Bayer, T. Möller, and B. von Issendorff, Phys. Rev. B **79**, 241102 (2009).
[17] A. Terasaki, T. Majima, and T. Kondow, J. Chem. Phys. **127**, 231101 (2007).
[18] S. Peredkov, A. Savci, S. Peters, M. Neeb, W. Eberhardt, H. Kampschulte, J. Meyer, M. Tombers, B. Hofferberth, F. Menges, and G. Niedner-Schatteburg, J. Electron Spectrosc. Relat. Phenom. **184**, 113 (2011).
[19] G. Gutsev and C. Bauschlicher, J. Phys. Chem. A **107**, 4755 (2003).
[20] O. Šipr and H. Ebert, Phys. Rev. B **72**, 134406 (2005).
[21] R. Wu and A. J. Freeman, Phys. Rev. Lett. **73**, 1994 (1994).
[22] C. P. Bean and J. D. Livingston, J. Appl. Phys. **30**, S120 (1959).
[23] G. Rollmann, P. Entel, and S. Sahoo, Comput. Mater. Sci. **35**, 275 (2006).
[24] R. Singh and P. Kroll, Phys. Rev. B **78**, 245404 (2008).
[25] O. Diéguez, M. M. G. Alemany, C. Rey, P. Ordejón, and L. J. Gallego, Phys. Rev. B **63**, 205407 (2001).
[26] P. Bobadova-Parvanova, K. A. Jackson, S. Srinivas, M. Horoi, C. Köhler, and G. Seifert, J. Chem. Phys. **116**, 3576 (2002).
[27] G. L. Gutsev and C. W. Bauschlicher, J. Phys. Chem. A **107**, 7013 (2003).
[28] M. L. Tiago, Y. Zhou, M. M. G. Alemany, Y. Saad, and J. R. Chelikowsky, Phys. Rev. Lett. **97**, 147201 (2006).
[29] J. Stöhr and H. König, Phys. Rev. Lett. **75**, 3748 (1995).
[30] G. H. O. Daalderop, P. J. Kelly, and M. F. H. Schuurmans, Phys. Rev. B **41**, 11 919 (1990).
[31] P. Błoński and J. Hafner, Phys. Rev. B **79**, 224418 (2009).
[32] P. Bobadova-Parvanova, K. A. Jackson, S. Srinivas, and M. Horoi, Phys. Rev. B **66**, 195402 (2002).
[33] B. I. Dunlap, Phys. Rev. A **41**, 5691 (1990).